iScience

CellPress
OPEN ACCESS

Article

Transcriptional upregulation of MAPK15 by NF-κB signaling boosts the efficacy of combination therapy with cisplatin and TNF-α

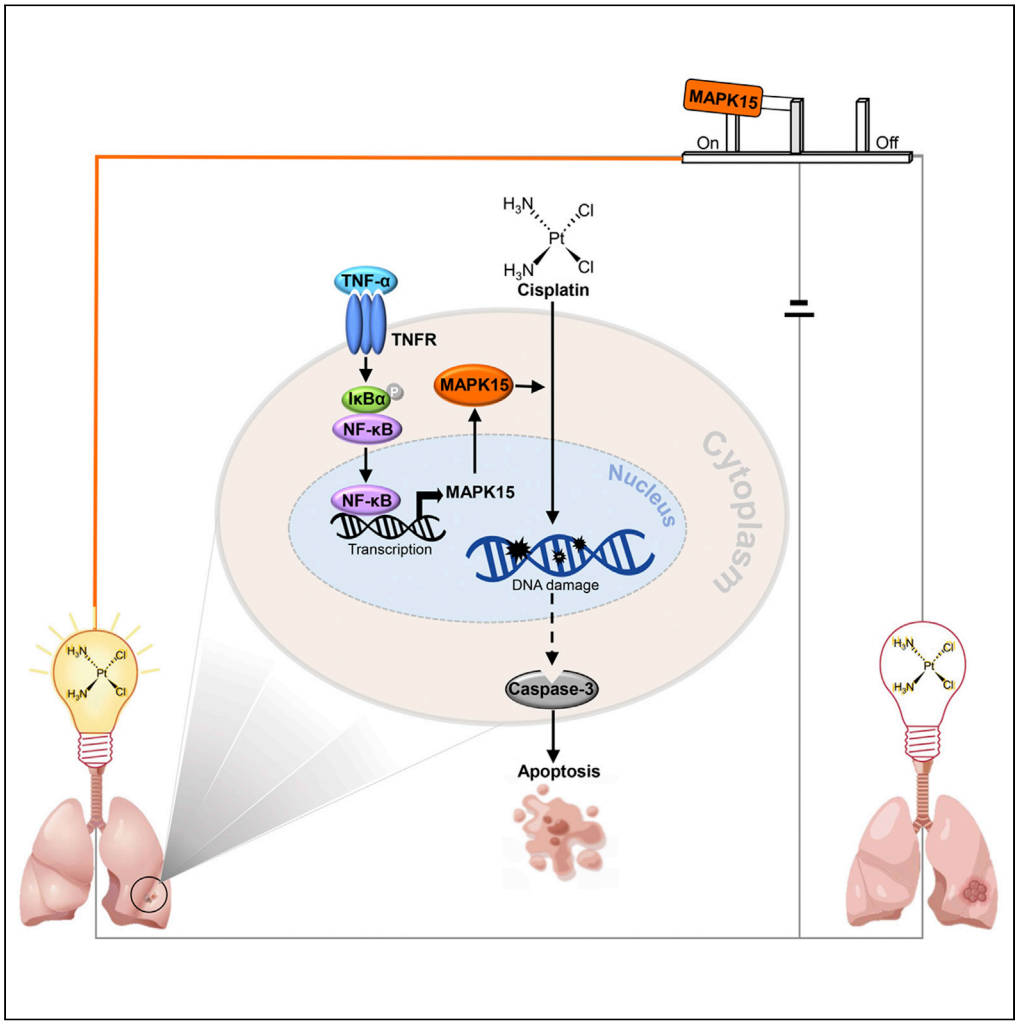

Dan-Dan Wu, Li-Juan Dai, Heng Wee Tan, ..., Sheng-Qing Li, Andy T.Y. Lau, Yan-Ming Xu

andytylau@stu.edu.cn (A.T.Y.L.)
amyymxu@stu.edu.cn (Y.-M.X.)

Highlights

TNF-α-activated NF-κB signaling initiates the transcriptional regulation of MAPK15

MAPK15 is essential for TNF-α-augmented cisplatin-induced cell apoptosis

Elevating MAPK15 expression can be a new strategy to improve the efficacy of cisplatin

Wu et al., iScience 25, 105459
December 22, 2022
https://doi.org/10.1016/j.isci.2022.105459

iScience

CellPress
OPEN ACCESS

Article

Transcriptional upregulation of MAPK15 by NF-κB signaling boosts the efficacy of combination therapy with cisplatin and TNF-α

Dan-Dan Wu,[1,4] Li-Juan Dai,[1,4] Heng Wee Tan,[1] Xiao-Yun Zhao,[1] Qi-Yao Wei,[1] Qiu-Hua Zhong,[1] Yan-Chen Ji,[1] Xiao-Hui Yin,[1] Fei-Yuan Yu,[1] Dong-Yan Jin,[2] Sheng-Qing Li,[3] Andy T.Y. Lau,[1,*] and Yan-Ming Xu[1,5,*]

SUMMARY

The efficacy of cisplatin in treating advanced non-small cell lung cancer is limited mainly because of insensitivity and/or acquired resistance. MAPK15, previously shown by us to enhance the sensitivity of the anti-cancer drug arsenic trioxide, could also enhance the sensitivity of other anti-cancer drugs. Here, we explore the potential role of MAPK15 in chemosensitivity to cisplatin in human lung cancer cells. Our results indicated that the expression level of MAPK15 was positively correlated with cisplatin sensitivity through affecting the DNA repair capacity of cisplatin-treated cells. The expression of MAPK15 was transcriptionally regulated by the TNF-α-activated NF-κB signaling pathway, and TNF-α synergized with cisplatin, in a MAPK15-dependent manner, to exert cytotoxicity *in vitro* and *in vivo*. Therefore, levels of TNF-α dictate the responsiveness/sensitivity of lung cancer cells to cisplatin by transcriptionally upregulating MAPK15 to enhance chemosensitivity, suggesting manipulation of MAPK15 as a strategy to improve the therapeutic efficacy of chemotherapeutic drugs.

INTRODUCTION

Lung cancer is the most commonly diagnosed cancer and is characterized as one of the leading causes of cancer-related death worldwide (Bray et al., 2018; Miller et al.,2019). Platinum-based chemotherapies are commonly used as first-line drugs in the treatment of various human cancers, in particular, advanced non-small cell lung cancer (NSCLC) (Sullivan et al., 2014; Fennell et al., 2016; Dasari and Tchounwou, 2014). Cisplatin is a platinum-based drug that mainly interacts with DNA to form intrastrand and interstrand cross-linking adducts, activating multiple signal transduction pathways in cells, including protein kinase C, p53, AKT, mitogen-activated protein kinase (MAPK), and apoptosis-related proteins, which eventually leads to cell apoptosis (Dasari and Tchounwou, 2014; Galluzzi et al., 2014). However, the efficacy of cisplatin is limited in clinical application mainly because of the insensitivity and/or acquired resistance of tumor cells. Researchers have reported the mechanism of acquired resistance to cisplatin is mainly comprised of reduced drug absorption, increased drug inactivation, inhibition of apoptosis, and repair of DNA adducts (Galluzzi et al., 2012). To overcome this, combined treatment using cisplatin with other drugs, and modification of existing cisplatin-based treatments, have been applied to increase the sensitivity of cisplatin toward cancer cells, suggesting the potential improvements for cisplatin-based combination chemotherapy.

Although studies have shown that the MAPK pathways, which consist of extracellular signal-regulated kinase (ERK), c-Jun N-terminal kinase (JNK), and p38 MAPK pathways, are activated after cisplatin treatment, it is still unclear whether the activation of these pathways prevents or contributes to cisplatin-induced apoptosis (Dasari and Tchounwou, 2014; Achkar et al.,2018). Among the MAPKs, which comprise a superfamily of serine/threonine protein kinases, MAPK15 is the most recently identified and least studied member of the MAPK family (Abe et al., 2002). MAPK15 is also known as extracellular signal-regulated kinase 7 or 8 (ERK7/8) and it possesses a typical Thr-Glu-Tyr motif in the activation loop of the kinase domain, which can be activated by auto-phosphorylation, yet, the existence of an upstream kinase is unknown (Lau and Xu, 2019). In addition, the kinase activity of MAPK15 can be activated by serum, DNA damage, and human oncogenes (Abe et al., 2002; Klevernic et al., 2006, 2009; Iavarone et al., 2006), and in turn controls the activity of several nuclear receptors, such as androgen receptor, glucocorticoid receptors, and estrogen-related receptor α (Rossi et al., 2011; Saelzler et al., 2006; Henrich et al., 2003).

[1]Laboratory of Cancer Biology and Epigenetics, Department of Cell Biology and Genetics, Shantou University Medical College, Shantou 515041, People's Republic of China

[2]School of Biomedical Sciences, Li Ka Shing Faculty of Medicine, The University of Hong Kong, Hong Kong, People's Republic of China

[3]Department of Pulmonary and Critical Care Medicine, Huashan Hospital, Fudan University, Shanghai 200040, People's Republic of China

[4]These authors contributed equally

[5]Lead contact

*Correspondence: andytylau@stu.edu.cn (A.T.Y.L.), amyymxu@stu.edu.cn (Y.-M.X.)

https://doi.org/10.1016/j.isci.2022.105459

Currently, studies have shown that MAPK15 plays an important role in regulating cell proliferation and transformation, apoptosis, autophagy, cell division, ciliogenesis, protein secretion, genome stability, and drug sensitivity (Lau and Xu, 2019). Thus, MAPK15 is likely associated with human cancers and is considered as an attractive target for cancer therapy. More detailed information about all known functions of MAPK15 and its potential as a druggable target is discussed in our review article (Lau and Xu, 2019). Intriguingly, our previous study has shown that MAPK15 enhances the sensitivity of NSCLC to arsenic trioxide (As_2O_3), an anti-cancer drug (Wu et al., 2017a). Notably, As_2O_3-activated MAPK15 further phosphorylates NF-κB inhibitor IκBα, which leads to IκBα ubiquitin-mediated proteasomal degradation. The release of NF-κB activates subsequent transcriptional regulation of apoptosis-related genes, resulting in As_2O_3-induced cell apoptosis. Given the potential role of MAPK15 in drug sensitivity for the chemotherapy of NSCLC, we next explored whether MAPK15 is involved in the chemosensitivity of the clinical first-line drug cisplatin.

Here, we provide evidence to show that the expression level of MAPK15 correlates with cisplatin sensitivity *in vitro* and *in vivo* through affecting the DNA repair capacity of cells exposed to cisplatin. Importantly, we found that the expression of MAPK15 can be transcriptionally regulated by the TNF-α-activated NF-κB signaling pathway, and the addition of TNF-α can synergize with cisplatin to enhance antitumor activity *in vitro* and *in vivo*. Our findings suggest that MAPK15 expression level is a critical determinant of cisplatin responsiveness in lung cancer.

RESULTS

MAPK15 expression levels correlate with the extent of cisplatin-induced cell apoptosis

We previously showed that MAPK15 enhances the sensitivity of NSCLC to As_2O_3 through the activation of NF-κB signaling (Wu et al., 2017a). So, we investigated whether MAPK15 is involved in the chemosensitivity of NSCLC to cisplatin. We engineered human H1299 lung cancer cells with stable knockdown (shMAPK15) or ectopic overexpression (pcDNA4-MAPK15) of MAPK15 and treated the cells with different doses of cisplatin. Intriguingly, knockdown of MAPK15 attenuated the cell death induced by cisplatin compared with the scrambled control (Figure 1A), whereas overexpression of MAPK15 significantly enhanced cell death compared to its empty vector control (Figure 1B). As the anti-cancer action of cisplatin mainly results from its ability to promote DNA damage-induced apoptosis (Galluzzi et al., 2012), we characterized the activation of the intrinsic apoptosis marker caspase-3 following cisplatin treatment. Cleaved caspase-3 was increased in a dose-dependent course (Figure 1C), suggesting that treatment of cisplatin leads to cell apoptosis in a dose-dependent manner (Figure S1). These results indicate that MAPK15 is involved in the cisplatin sensitivity of lung cancer cells as evidenced by the fact that the expression of MAPK15 enhances cisplatin-induced apoptosis in H1299 cells.

We further investigated the role of MAPK15 in cisplatin tolerance of lung cancer cells *in vivo* in a tumor xenograft model. Tumor volume was measured at 31 days after inoculation of H1299 cells stably overexpressing MAPK15 and control H1299 cells in the two flanks of each mouse. Overexpression of MAPK15 not only inhibited tumor formation when compared with the empty vector control (Figure 1D), but also was more sensitive to cisplatin-mediated tumor growth inhibition (Figure 1E). Taken together, these results suggest that the expression of MAPK15 enhances cisplatin sensitivity both *in vitro* and *in vivo*.

MAPK15 expression is transcriptionally regulated by NF-κB and enhanced by TNF-α

Given that MAPK15 is involved during the course of apoptosis induced by cisplatin, we sought to induce the expression of MAPK15 via transcriptional regulation to sensitize lung cancer to cisplatin. Our previous studies showed that MAPK15 could mediate the activation of NF-κB signaling pathway through the phosphorylation of IκBα (Wu et al., 2017a), and we speculated that NF-κB, as a transcription factor, might in turn regulate the expression of MAPK15 in a feedback mechanism. To verify this hypothesis, by using the JASPAR website, we first identified four predicted NF-κB transcriptional binding sites (TBSs) in the MAPK15 promoter region (Figures 2A, S2, and Table S1). Chromatin immunoprecipitation (ChIP) assay, using NF-κB p65 antibody, was performed to validate the *in vivo* binding of NF-κB to the MAPK15 promoter. Agarose gel electrophoresis results showed that the predicted site-4 (TBS4) was specifically precipitated with NF-κB p65 antibody, whereas no binding was observed in the IgG control (Figure 2B), indicating that NF-κB p65 may bind to the promoter region of MAPK15 at TBS4 *in vivo*. Moreover, as it is well known that tumor necrosis factor alpha (TNF-α) can activate the NF-κB signaling pathway (Hayden and Ghosh, 2008), we determined whether TNF-α could affect NF-κB binding to the MAPK15 promoter. ChIP assay showed that, compared with untreated control, TNF-α stimulation increased the binding of p65 to the

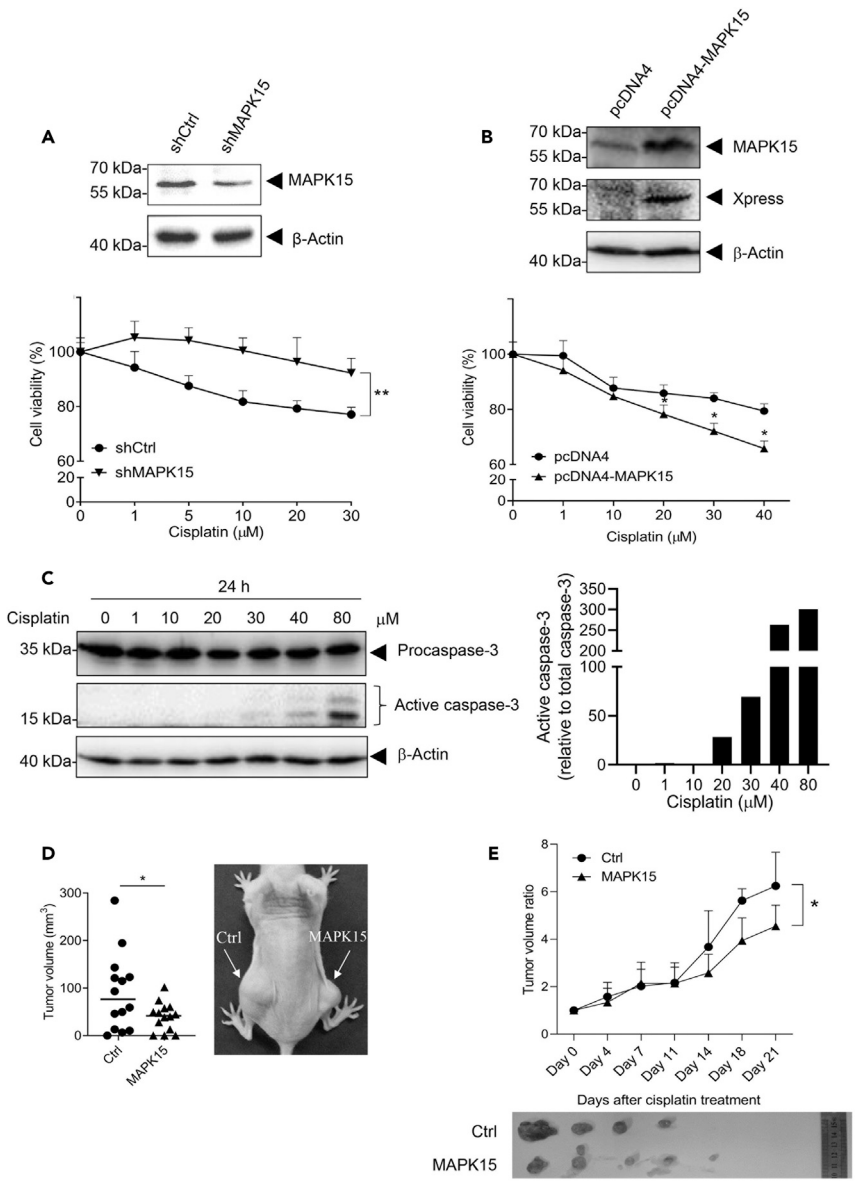

Figure 1. MAPK15 expression levels correlate with the extent of cisplatin-induced cell apoptosis

(A and B) Expression of MAPK15 in MAPK15 knockdown (A) or MAPK15 overexpressing (B) H1299 stable cell lines were detected by immunoblot assay using MAPK15 antibody and anti-Xpress tag antibody, and β-actin was used as the loading control. The cells were sham-exposed or exposed to various doses of cisplatin for 24 h, and cell survival was determined by a naphthol blue black (NBB) staining assay. Cisplatin-exposed cells were normalized to the sham-exposed control (n = 3, mean ± SEM).

(C) H1299 cells were sham-exposed or exposed to 1–80 μM cisplatin for 24 h. Cells were lysed and subjected to immunoblot analysis with antibodies against caspase-3. The membrane was stripped and reprobed with β-actin to ensure equal loading of samples. The gray intensities of active caspase-3 were normalized to total caspase-3. See also Figure S1.

(D) H1299 cells stably expressing MAPK15 or control empty vector were separately injected into the two flanks of each mouse (n = 14, mean ± SEM), as indicated by arrows on the right panel. Left panel: final average tumor size. Right panel: representative photograph of a mouse 31 days after cell injection.

(E) Tumor xenografts were formed from H1299 cells implanted into nude mice (n = 5 for stably expressing MAPK15 cells, n = 4 for the control group, mean ± SEM). Top panel: Tumor volume was measured after cisplatin treatment (3.5 mg/kg) at the indicated time points. Bottom panel: Images of excised tumor nodules isolated after cisplatin treatment for 21 days. Two-way ANOVA was used to analyze data in (A) and (E); a *t*-test was used to analyze data in (B) and (D). Significant differences are indicated as *p< 0.05 or **p< 0.01.

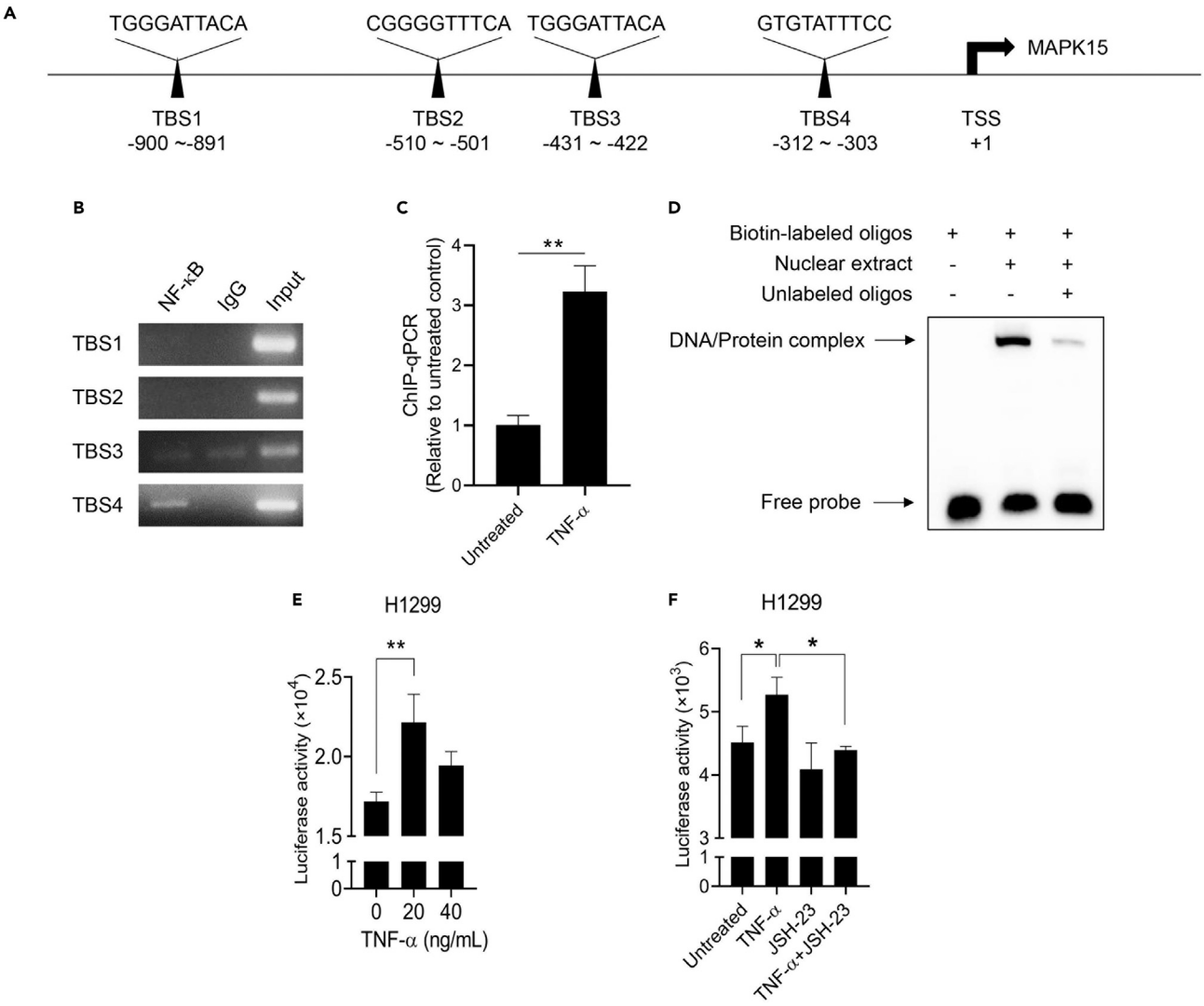

Figure 2. Transcriptional regulation of MAPK15 expression by NF-κB

(A) MAPK15 promoter landscape with putative NF-κB binding sites. Triangles represent the four predicted NF-κB binding sites, named TBS1, TBS2, TBS3, and TBS4, in the MAPK15 promoter region, and their distances from the transcription start site (TSS). See also Figure S2, Tables S1, and S2.

(B) ChIP analysis of the *in vivo* binding of NF-κB to the MAPK15 promoter. After purification of the DNA-p65 complex immunoprecipitated by p65 antibody, PCR was performed using purified DNA as template and the PCR products were subjected to 1% agarose gel electrophoresis.

(C) H1299 cells were sham-exposed or exposed to 20 ng/mL TNF-α for 12 h, then DNA binding to p65 protein was examined by ChIP-qPCR (n = 3, mean ± SEM, unpaired *t*-test). See also Figure S3.

(D) *In vitro* binding of NF-κB to the MAPK15 promoter determined by EMSA. H1299 cells were transiently transfected with pCMV-p65. At 24 h after transfection, nuclear protein was isolated and subjected to EMSA with biotin-labeled oligos corresponding to site 4 (TBS4).

(E) TNF-α stimulation enhances MAPK15 promoter activity. H1299 cells were transiently transfected with the pJC6-GL3-5×MAPK15-firefly luciferase reporter plasmid and pRL-sv40-*Renilla* plasmid. At 24 h post-transfection, cells were seeded into a 6-well plate and 24 h later, cells were sham-exposed or exposed to 20–40 ng/mL TNF-α for an additional 12 h. MAPK15 luciferase activity was measured and normalized to *Renilla* luciferase activity (n = 3, mean ± SEM, one-way ANOVA). See also Figure S4.

(F) NF-κB inhibitor JSH-23 inhibits TNF-α-induced MAPK15 promoter activity. Same as (E), 24 h post-transfection, cells were pretreated with 30 μM JSH-23 for 4 h, and then co-treated with 20 ng/mL TNF-α for another 12 h (n = 3, mean ± SEM, one-way ANOVA). Significant differences are indicated as *p<0.05 or **p<0.01.

MAPK15 promoter (Figures 2C and S3). To further determine whether NF-κB p65 binds to the MAPK15 promoter at TBS4 *in vitro*, electrophoretic mobility shift assay (EMSA) was conducted by incubating biotin-labeled double-stranded TBS4 oligonucleotides with nuclear extracts from H1299 cells transfected with a pCMV-p65 plasmid. The biotin-labeled probe formed strong sequence-specific DNA-protein complexes

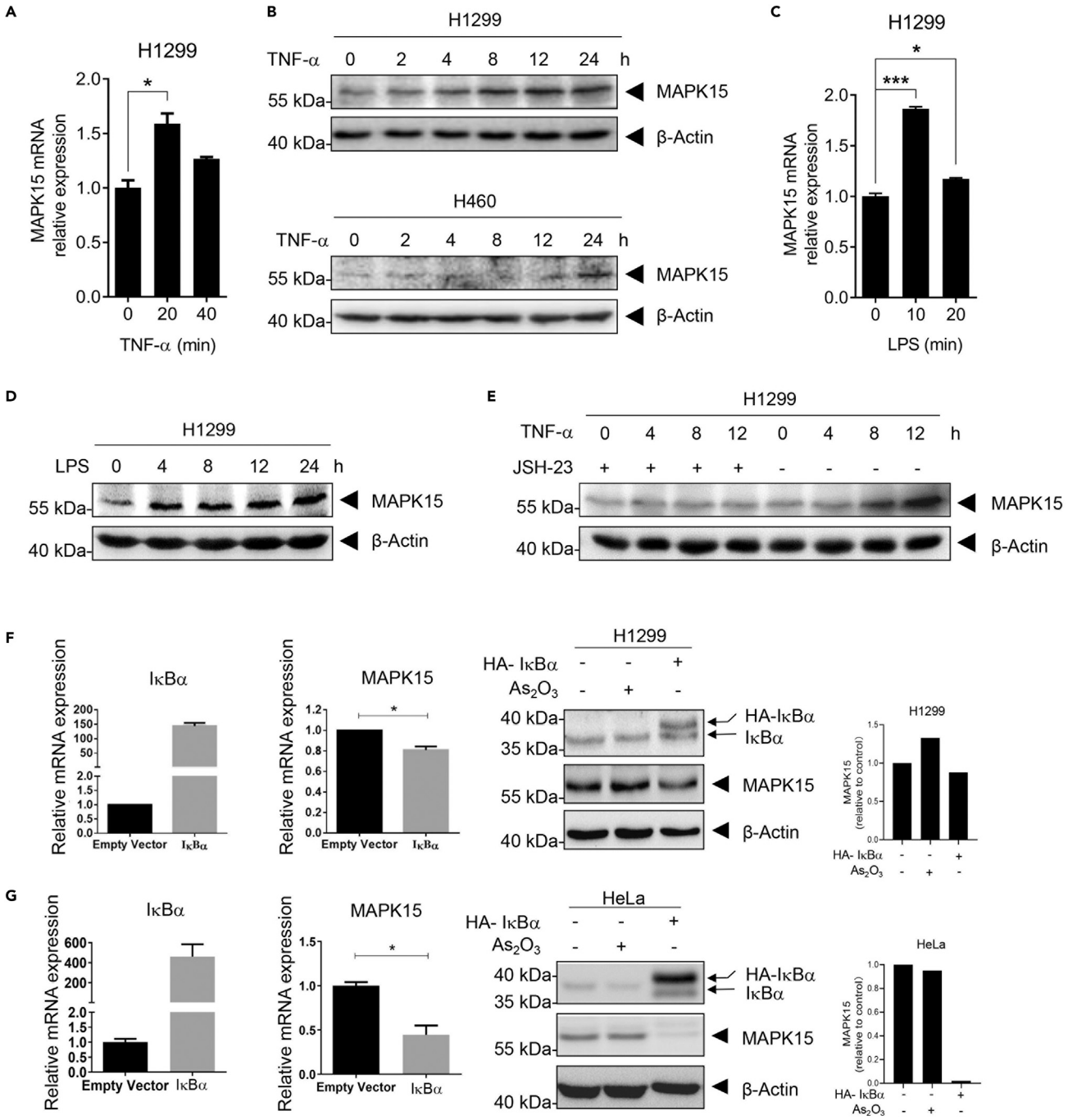

Figure 3. TNF-α and LPS induce MAPK15 expression through NF-κB signaling

(A and B) TNF-α stimulates the expression of MAPK15 in mRNA and protein levels. (A) H1299 cells were sham-exposed or exposed to 20 ng/mL TNF-α for 20 to 40 min, qRT-PCR was used to determine the mRNA level of MAPK15 (n = 3, mean ± SEM, one-way ANOVA). (B) H1299 and H460 cell lines were sham-exposed or exposed to 20 ng/mL TNF-α for 2 to 24 h, Immunoblot analysis was performed to detect the protein expression of MAPK15. β-Actin was used to monitor loading differences. See also Figure S3.

(C and D) LPS induces MAPK15 mRNA and protein expression. H1299 cells were sham-exposed or exposed to 1 μg/mL LPS for 10 to 20 min (C) or for 4 to 24 h (D) qRT-PCR was used to determine the mRNA level of MAPK15 (n = 3, mean ± SEM, one-way ANOVA). Immunoblot analysis was performed to detect the protein expression of MAPK15 using antibody against MAPK15. β-Actin was used to monitor loading differences. The data are representative of three independent experiments. Significant differences are indicated as *p<0.05 or ***p<0.001.

Figure 3. *Continued*

(E) JSH-23 inhibits TNF-α-induced upregulation of MAPK15 expression. H1299 cells were sham-exposed or exposed to 30 μM JSH-23 for 4 h, and then challenged with or without 20 ng/mL TNF-α for 4 to 12 h, then MAPK15 expression was detected by immunoblot assay. β-Actin was used to monitor loading differences.

(F and G) Overexpression of NF-κB inhibitor IκBα represses the expression of MAPK15. H1299 (F) and HeLa (G) cells were transiently transfected with pCMV4-3HA/IκBα or empty vector. At 24 h post-transfection, cells were harvested and qRT-PCR was used to assess the mRNA expression, and immunoblot assay was performed to detect the protein expression of IκBα, MAPK15, and β-actin (n = 3, mean ± SEM, unpaired *t*-test). As_2O_3 treatment was used as a positive control for the degradation of IκBα. Significant differences were analyzed by the unpaired *t*-test, *p<0.05. See also Figure S5.

with p65-transfected nuclear extracts. Competition with an extra 200-fold unlabeled TBS4 probe resulted in a reduction of biotin-labeled DNA-protein complexes (Figure 2D). Therefore, these results indicate that NF-κB p65 binds to the promoter of MAPK15 at TBS4 *in vitro* and *in vivo*.

Next, a dual-luciferase assay was performed to further investigate whether the binding of p65 to MAPK15 promoter can enhance the MAPK15 promoter activity. A luciferase reporter gene, containing five repeats of the TBS4 sequence in the promoter (pJC6-GL3-5×MAPK15-firefly), was constructed. As shown in Figures 2E and 2F, stimulation with TNF-α enhanced MAPK15 promoter activity, and this enhanced activity could be inhibited by either the NF-κB inhibitor JSH-23 or mutating TBS4 (Figure S4). Collectively, these results show that MAPK15 promoter activity could be enhanced by TNF-α treatment and specifically associated with NF-κB activation.

TNF-α induces MAPK15 expression through NF-κB signaling

Based on the results that TNF-α treatment enhanced MAPK15 promoter activity, TNF-α was then applied to stimulate MAPK15 expression in H1299 cells and two other NSCLC cell lines (H460 and H358). TNF-α treatment induced MAPK15 mRNA and protein expression in H1299 and H460 cells in a time-dependent manner (Figures 3A and 3B). However, in another NSCLC cell line H358, although binding of NF-κB at the MAPK15 promoter was observed, no induction of MAPK15 expression by TNF-α occurred (Figure S3). As bacterial lipopolysaccharide (LPS) can induce the expression of TNF-α (Hayden and Ghosh, 2008), and LPS is commonly used as an activator of NF-κB signaling, we determined the expression of MAPK15 following stimulation with LPS. Upregulation of MAPK15 mRNA and protein expression was also found in H1299 cells upon LPS treatment (Figures 3C and 3D). Furthermore, JSH-23 suppressed TNF-α-induced upregulation of MAPK15 expression (Figure 3E), indicating that MAPK15 expression is upregulated by TNF-α through a mechanism dependent on NF-κB in lung cancer cells. Similarly, ectopic overexpression of IκBα, an NF-κB inhibitor, significantly suppressed the mRNA and protein levels of MAPK15 in H1299 and HeLa cells (Figures 3F, 3G, and S5). Altogether, our results reveal that TNF-α upregulates MAPK15 expression through a mechanism dependent on NF-κB.

TNF-α augments chemosensitivity of lung cancer cells to cisplatin

The results here thus far have demonstrated that TNF-α induces the expression of MAPK15, which is involved in the sensitivity to cisplatin. Thus, we investigated the possibility of improving the efficacy of cisplatin by combined treatment with TNF-α. The combination of TNF-α and cisplatin caused greater cell death of H1299 cells than cisplatin alone. TNF-α alone did not induce cytotoxicity (Figures 4A, S6, and S7). Similar results were obtained with H460 cells (Figures 4B and S7). Moreover, immunoblot assays showed that the combination of TNF-α and cisplatin increased the cleavage of apoptosis mediators-caspase-3 and PARP1 both in H1299 and H460 cells (Figures 4C and 4D). Surprisingly, no augmentation of cell sensitivity was observed in H358 cells on co-treatment of TNF-α with cisplatin (Figure S8). Our data indicate that TNF-α and cisplatin synergistically induce apoptosis in lung cancer cell lines H1299 and H460. A H1299 cell nude mouse xenograft model was established to determine whether TNF-α enhanced cisplatin sensitivity *in vivo*. As shown in Figure 4E, the combined treatment of TNF-α and cisplatin inhibited tumor growth to a greater extent than cisplatin treatment alone.

MAPK15 is critical for TNF-α-augmented chemosensitivity of H1299 cells to cisplatin

To determine whether the enhancement of cisplatin chemosensitivity of lung cancer cells by TNF-α depends on the expression of MAPK15, H1299 cells with stably knocked down MAPK15 were pretreated with TNF-α and then co-treated with various doses of cisplatin. When compared with cisplatin alone, intense cytotoxicity was observed following co-treatment of TNF-α with cisplatin in the shCtrl H1299 cells, which was not found in the shMAPK15 cells (Figures 5A and S9). Moreover, cleavage of both caspase-3 and

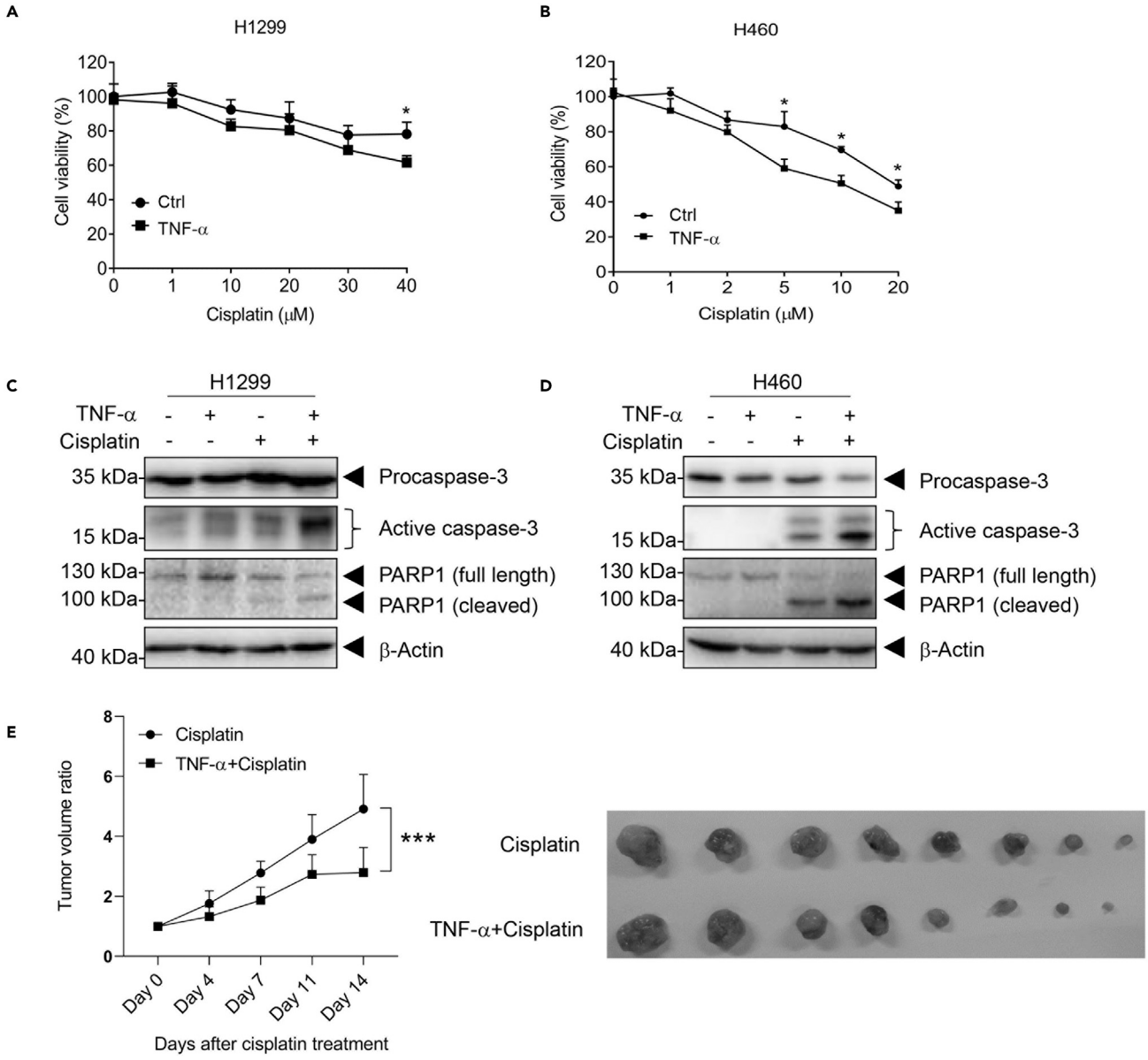

Figure 4. TNF-α augments cisplatin-induced lung cancer cell apoptosis

(A and B) Lung cancer cell lines H1299 (A) and H460 (B) were sham-exposed or exposed to 20 ng/mL TNF-α for 12 h, then co-treated with or without indicated cisplatin for 24 h. Cell viability was measured by NBB staining. Cisplatin-exposed cells were normalized to the sham-exposed control (n = 4, mean ± SEM, multiple *t*-test). See also Figures S6 and S7.

(C and D) Cells were treated the same as described in (A, B), H1299 (C), and H460 (D) cells were harvested, lysed, and protein extracts were subjected to immunoblot assay with antibodies against caspase-3 and PARP1, and β-actin was used as the internal control. The data are representative of three independent experiments. See also Figure S8.

(E) TNF-α promotes cisplatin sensitivity *in vivo*. Tumor xenografts were formed from H1299 cells implanted in nude mice (n = 8 for each group, mean ± SEM, two-way ANOVA). Left panel: tumor volume was measured after TNF-α (20 ng) combined with cisplatin or cisplatin alone treatment (3.5 mg/kg). Right panel: images of excised tumor nodules. Significant differences are indicated as *p<0.05 or ***p<0.001.

PARP1 was elevated in shCtrl H1299 cells, especially following combined treatment of TNF-α and cisplatin, but was not observed in shMAPK15 cells (Figure 5B).

To explore whether cisplatin-induced cell apoptosis resulted from cell-cycle arrest, cell cycle distribution following cisplatin treatment was assessed. Notably, compared with the cisplatin alone group, a pronounced increase in the sub G0/G1 population was found after co-treatment with TNF-α and cisplatin in

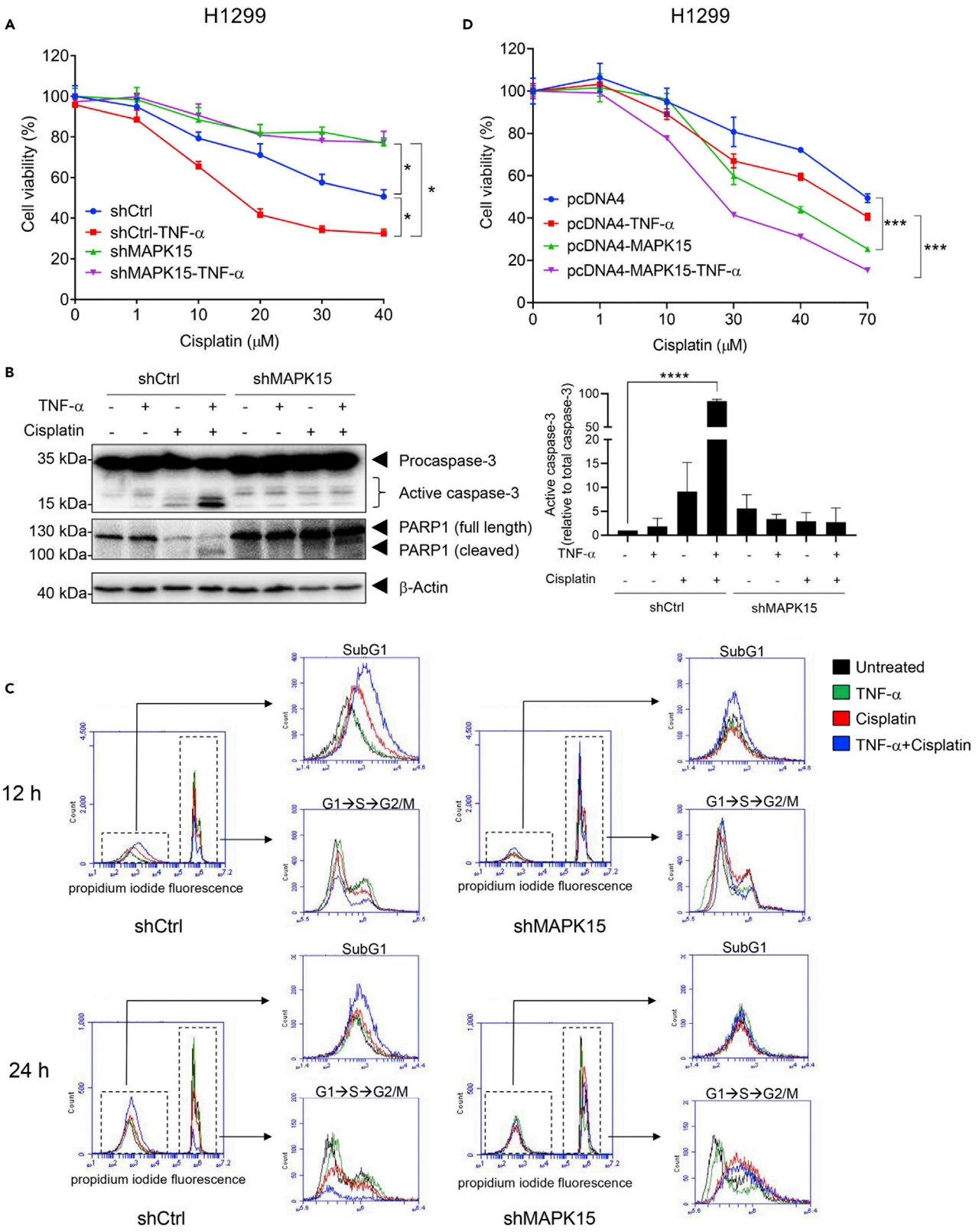
A
H1299
Cell viability (%)
Cisplatin (μM)
shCtrl
shCtrl-TNF-α
shMAPK15
shMAPK15-TNF-α
D
H1299
pcDNA4
pcDNA4-TNF-α
pcDNA4-MAPK15
pcDNA4-MAPK15-TNF-α
B
shCtrl
shMAPK15
TNF-α
Cisplatin
35 kDa
15 kDa
130 kDa
100 kDa
40 kDa
Procaspase-3
Active caspase-3
PARP1 (full length)
PARP1 (cleaved)
β-Actin
Active caspase-3 (relative to total caspase-3)
****
C
12 h
24 h
SubG1
G1→S→G2/M
propidium iodide fluorescence
Untreated
TNF-α
Cisplatin
TNF-α+Cisplatin

Figure 5. MAPK15 is a critical molecule in TNF-α-augmented cisplatin sensitivity

(A) Knocking down MAPK15 abrogates TNF-α-augmented cisplatin sensitivity of H1299 cells. MAPK15 stable knockdown and control H1299 cells were sham-exposed or exposed to 20 ng/mL TNF-α for 12 h, then co-treated with or without 1–40 μM cisplatin for 24 h. Cell viability was determined by NBB staining (n = 5, mean ± SEM, two-way ANOVA). See also Figure S9.

(B) Treatment was as described in (A). Cells were harvested and lysed for protein detection via immunoblot assay using antibodies against caspase-3, PARP1, and β-actin. The gray intensities of active caspase-3 were normalized to total caspase-3 (n = 3, mean ± SEM, one-way ANOVA).

(C) Knockdown of MAPK15 causes G2/M-phase arrest. After the same treatment as described in (A), cells were pretreated with TNF-α for 12 h, then co-treated with or without 40 μM cisplatin for 12 or 24 h. Cells were subjected to PI staining and analyzed by flow cytometry. Sub G0/G1 count is shown in the left panel and the counts of G1/S/G2/M phases are shown in the right panel.

(D) Overexpression of MAPK15 promotes TNF-α-augmented cisplatin-induced cell apoptosis. Stable MAPK15-expressing H1299 cells were challenged with 20 ng/mL TNF-α for 12 h, then co-treated with or without 1–70 μM cisplatin for 24 h. Cisplatin-exposed cells were normalized to the sham-exposed control (n = 5, mean ± SEM, two-way ANOVA). Significant differences are indicated as *p<0.05, ***p<0.001, or ****p<0.0001.

the shCtrl H1299 cells, but not in the shMAPK15 cells (Figure 5C). Nevertheless, an increased G2/M arrest was observed in shMAPK15 cells following co-treatment with TNF-α and cisplatin, or treatment with cisplatin alone, for 24 h, compared with untreated control Figure 5C), indicating that G2/M arrest might enable MAPK15 knockdown H1299 cells to survive upon cisplatin treatment. These results demonstrate that knockdown of MAPK15 blunts TNF-α-augmented cisplatin-induced cell apoptosis.

On the other hand, the combined treatment with TNF-α and cisplatin was also used to treat stably overexpressing MAPK15 and control H1299 cells. TNF-α-augmented cisplatin-induced cell apoptosis, to some extent, in both overexpressing MAPK15 and corresponding control H1299 cells. Overexpression of MAPK15 further enhanced the cytotoxicity of combined treatment with TNF-α and cisplatin (Figure 5D). The above results imply that MAPK15 is essential for TNF-α-augmented chemosensitivity of lung cancer cells to cisplatin.

MAPK15 enhances TNF-α-augmented cisplatin-induced DNA damage

Since cisplatin blocks DNA replication and induces DNA damage and cell death by creating intrastrand and interstrand DNA crosslinks, we wondered whether MAPK15 promotes TNF-α-augmented cisplatin-induced apoptosis by affecting cisplatin-induced DNA damage. Gamma-H2AX (Ser139-phosphorylated H2AX) is widely used as a marker for DNA damage, because H2AX is rapidly phosphorylated in large chromatin domains flanking DNA double-strand breaks (Lu et al., 2006). Here, phosphorylation of H2AX increased with increasing doses of cisplatin (Figure 6A), whereas decreased phosphorylation of H2AX was detected in shMAPK15 cells when compared with shCtrl H1299 cells (Figure 6B). In addition, the expressions of p21 (a cyclin-dependent kinase inhibitor) and cleaved-RAD51 (a DNA damage marker) decreased in shMAPK15 H1299 cells on cisplatin treatment (Figure 6B). Notably, increased phosphorylation of H2AX and cleavage of RAD51 were observed in both H1299 and H460 cells following combined treatment with TNF-α and cisplatin, compared with the untreated, TNF-α alone, and cisplatin alone groups (Figure 6C). Moreover, increased p-H2AX and cleaved-RAD51 levels were detected in the shCtrl cells, especially on the co-treatment of TNF-α and cisplatin, whereas this was not observed in the shMAPK15 H1299 cells (Figure 6D). Furthermore, to explore the dynamics of cisplatin-induced DNA damage and apoptosis, H1299 cells were exposed to cisplatin alone or the combination of cisplatin and TNF-α for 12 or 24 h. The phosphorylation of H2AX and cleavage of RAD51 increased at 24 h post-treatment, compared with 12 h, as well as increased cleavage of caspase-3 (Figure 6E). The above findings suggest that the expression of MAPK15 is critical in the process of TNF-α-augmented cisplatin-induced DNA damage.

MAPK15 influences the DNA repair response post-cisplatin treatment

A comet assay was used to assess DNA crosslink formation and DNA repair capacity in MAPK15 knockdown or control H1299 cells in response to cisplatin. The tail extent moment decreased dramatically in both shMAPK15 and shCtrl H1299 cells when exposed to cisplatin (Figure 7A). However, we found that the tail extent moment was increased in the cisplatin-treated H1299 cells when measured 24 h post-cisplatin treatment (Figure 7B), probably because of DNA crosslink repair during the recovery period. Therefore, we again performed a comet assay in the MAPK15 knockdown and control H1299 cells, but this time with a 24 h recovery period post-cisplatin treatment, and the results showed that the tail extent moment increased in both shMAPK15 and shCtrl H1299 cells compared to the corresponding non-drug-treated control, with shMAPK15 H1299 cells showing a greater tail extent moment than the shCtrl cells (Figure 7C). These results indicate that the MAPK15 knockdown cells have a greater DNA repair capacity

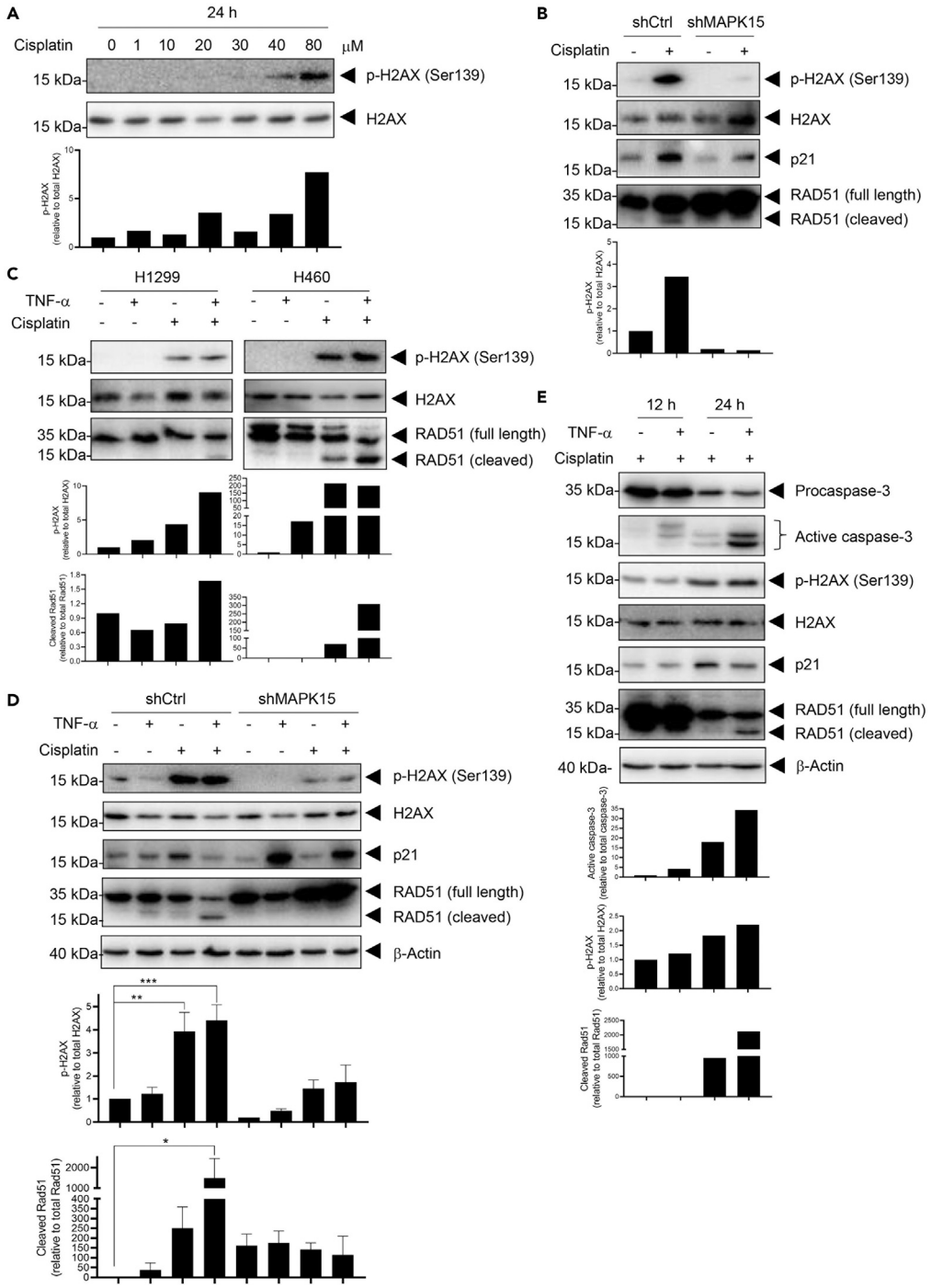

Figure 6. MAPK15 promotes TNF-α-augmented cisplatin-induced DNA damage

(A) Treatment same as in Figure 1C. Immunoblotting was performed to detect cisplatin-induced DNA damage using antibodies against p-H2AX (Ser139) and H2AX.

(B) Stable MAPK15 knockdown and control H1299 cells were sham-exposed or exposed to 40 μM cisplatin for 24 h. Immunoblotting was performed using antibodies against p-H2AX (Ser139), H2AX, p21, and RAD51.

(C) Same treatment as in Figures 4C and 4D. Immunoblot assay was performed using antibodies against p-H2AX (Ser139), H2AX, and RAD51.

(D) Same as in Figure 5B, DNA damage was detected by immunoblotting with antibodies against p-H2AX (Ser139), H2AX, p21, and RAD51 (n = 3, mean ± SEM, one-way ANOVA). Significant differences are indicated as *p<0.05, **p<0.01, or ***p<0.001.

Figure 6. *Continued*

(E) H1299 cells were sham-exposed or exposed to 20 ng/mL TNF-α for 12 h, then co-treated with 20 ng/mL TNF-α and 40 μM cisplatin or cisplatin alone for 12–24 h. Cells were harvested and lysed, and protein extracts were subjected to immunoblot assay using antibodies against caspase-3, p-H2AX (Ser139), H2AX, p21, and RAD51. β-Actin was used as the internal control. The gray intensity of the bands was quantified by Gelpro 32 software. The active caspase-3 was normalized to total caspase-3, cleaved RAD51 was normalized to total RAD51, and p-H2AX was normalized to total H2AX.

compared with the shCtrl cells, suggesting that MAPK15 affects the efficacy of cisplatin by inhibiting the cell's DNA repair capacity.

DISCUSSION

In this study, we sought to understand the role of MAPK15 in the chemosensitivity of lung cancer to cisplatin. Previously, in a cisplatin sensitivity study, MAPK3/1 (ERK1/2) was found to be activated by cisplatin, and the activation of ERK1/2 is the most critical mediator in cisplatin-induced apoptosis (Wang et al., 2000). Klevernic et al. have previously shown that the phosphorylation of MAPK15 can be induced by DNA-damaging agents (Klevernic et al., 2009), which we also have found for cisplatin (Figure S10). Here, we demonstrate for the first time that MAPK15 is involved in the chemosensitivity of lung cancer to cisplatin both *in vitro* and *in vivo*. Expression of MAPK15 enhances cisplatin-induced apoptosis in NSCLC cell lines by activating apoptosis-related proteins, suggesting that MAPK15 plays an important role in cisplatin-induced NSCLC cell apoptosis. In addition, we found that overexpression of MAPK15 attenuated tumor xenograft formation compared to empty vector control. However, this finding is inconsistent with our previous report that MAPK15 overexpression renders mouse skin cancer cell tumorigenesis *in vivo* (Xu et al., 2010). Possible reasons could be that the effect of MAPK15 in tumor formation may vary among cell lines of different cancer types (H1299 vs. JB6 Cl41) and the inoculation methods (two flanks of a mouse vs. one flank of each mouse).

As MAPK15 expression enhanced cell apoptosis induced by cisplatin, we tried to induce the expression of MAPK15 to sensitize human lung cancer cells to cisplatin. As our previous study showed that MAPK15 could activate NF-κB by phosphorylating IκBα (Wu et al., 2017a), we hypothesized that NF-κB might in turn regulate the expression of MAPK15 by a positive feedback mechanism. Thus, we first predicted NF-κB binding sites at the promoter region of MAPK15 (TBS1–TBS4). Our results revealed and validated the binding of NF-κB p65 to the promoter of MAPK15 at TBS4. We also observed TNF-α activates NF-κB signaling, and TNF-α increases MAPK15 expression in lung cell lines, which further demonstrates that TNF-α induces the transcriptional expression of MAPK15 via the activation of NF-κB signaling. Furthermore, treatment with the NF-κB-specific inhibitor JSH-23 inhibited TNF-α-induced MAPK15 expression, suggesting that MAPK15 expression is tightly associated with NF-κB activation. Although a similar trend of NF-κB p65 binding affinity was found in another NSCLC cell line H358, no induction of MAPK15 expression was obtained. One possible explanation for this finding is that TNF-α treatment stimulates the formation of different NF-κB heterodimers among different cancer cell lines (Oeckinghaus et al., 2011), and the underlying mechanism needs to be further explored. To our knowledge, this is the first report to reveal the transcriptional control of MAPK15 by NF-κB, particularly upon TNF-α stimulation. Notably, the upregulation of MAPK15 might phosphorylate IκBα, which leads to the degradation of IκBα and further activation of NF-κB signaling in a positive feedback loop between MAPK15–IκBα and TNF-α–NF-κB signaling.

Prior studies have suggested that TNF-α stimulation induces apoptosis via the activation of transcription factors such as NF-κB (Hayden and Ghosh, 2014). Given that TNF-α is able to promote the transcriptional expression of MAPK15, which promotes cisplatin sensitivity in lung cancer cell lines, we sought to investigate whether TNF-α promotes the efficacy of cisplatin. Our results not only indicate that TNF-α synergizes with cisplatin to cell apoptosis in two lung cancer cell lines studied, but also confirm TNF-α increases cisplatin sensitivity *in vivo*. This is also supported by other studies reporting that TNF-α sensitizes cisplatin-induced cell death in neuroblastoma cells (Galenkamp et al., 2015) and breast cancer cells (Wu et al., 2017b), even though TNF-α has been reported to be involved in cisplatin-induced nephrotoxicity by inducing inflammation (Zhang et al., 2007; Ramesh and Reeves, 2003; Ramesh and Reeves, 2002; Benedetti et al., 2013). High doses of cisplatin treatment lead to severe renal failure because of the release of cytokines (Zhang et al., 2007; Ramesh and Reeves, 2003), but co-treatment with TNF-α enhances cisplatin-induced cell death at low doses of cisplatin (Galenkamp et al., 2015; Wu et al., 2017b). It is also important to mention that Benedetti et al. reported that combined treatment of cisplatin and

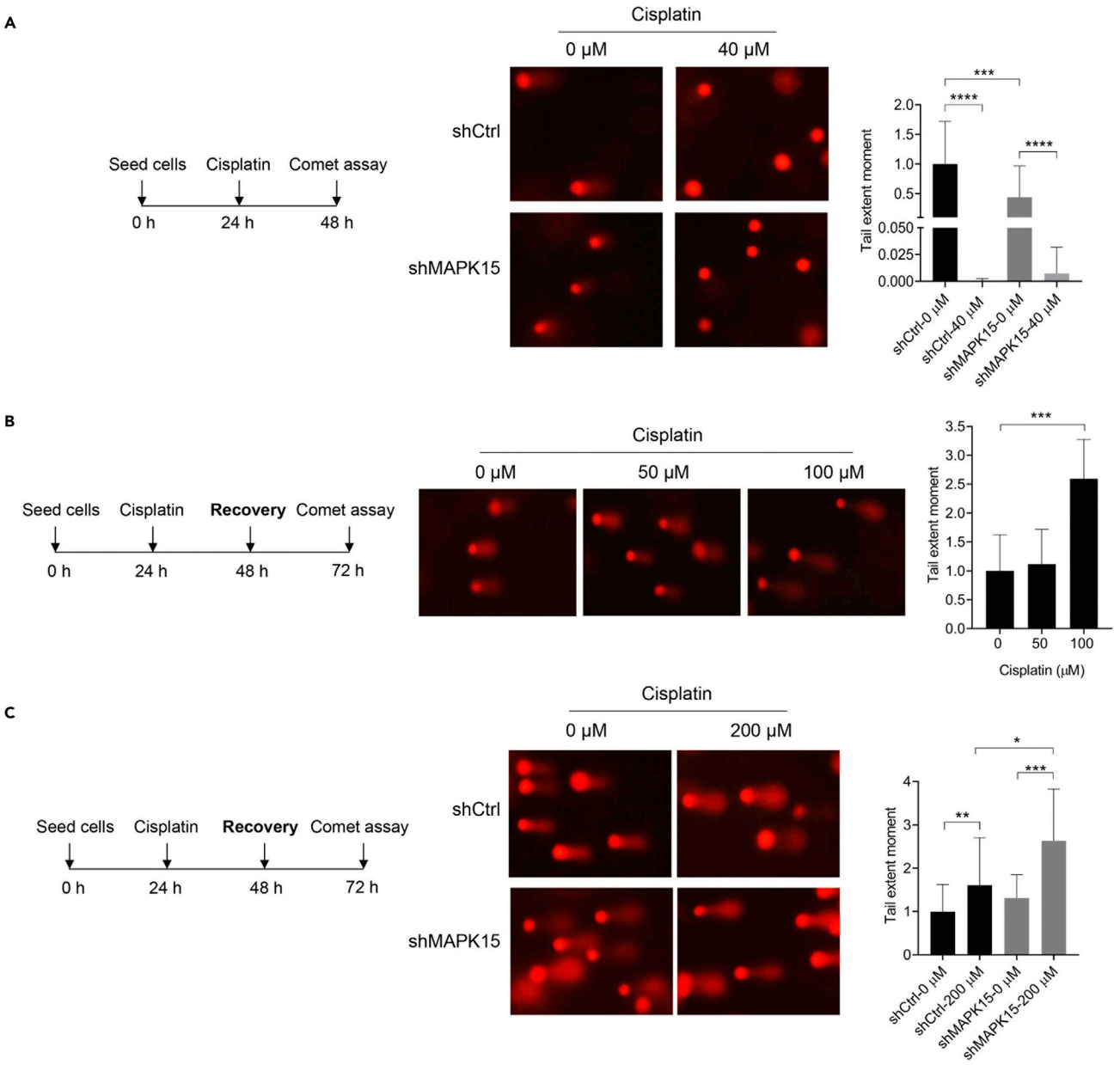

Figure 7. DNA repair capacity of MAPK15 knockdown H1299 cells exposed to cisplatin

(A) Stable MAPK15 knockdown and control H1299 cells were sham-exposed or treated with cisplatin for 24 h, and DNA damage of cells was detected by comet assay.

(B) DNA repair capacity of H1299 cells exposed to different doses of cisplatin. H1299 cells were sham-exposed or exposed to 50–100 μM cisplatin for 24 h, and culture medium was replaced with complete growth medium for another 24 h. DNA repair capacity of cells was assessed by comet assay.

(C) Stable MAPK15 knockdown and control H1299 cells were sham-exposed or treated with cisplatin for 24 h, and media was replaced with complete growth medium for another 24 h. (A–C) Representative images of cells stained with 5 μg/mL propidium iodide after gel electrophoresis and DNA damage magnitude (tail extent moment) are shown (n = 3, mean ± SEM, one-way ANOVA). Significant differences are indicated as *p<0.05, **p<0.01, ***p<0.001, or ****p<0.0001.

TNF-α inhibits the activation of NF-κB signaling, but leads to prolonged JNK and c-Jun phosphorylation (Benedetti et al., 2013). Since it has been shown that higher levels of cytokines and immune molecules (e.g., TNF-α) are present in the tumor microenvironment of patients, the levels of TNF-α could dictate the responsiveness/sensitivity of cancer cells to chemotherapeutic drugs. Our research shows that TNF-α-induced upregulation of MAPK15 expression is essential for the synergistic effect of TNF-α and cisplatin

on cell apoptosis. Furthermore, we observed that cell lines with TNF-α-induced upregulation of MAPK15 expression displayed TNF-α-augmented cisplatin-induced cell apoptosis. In addition, MAPK15 is required for TNF-α-augmented cisplatin-induced cell apoptosis. This may explain why TNF-α fails to enhance the anti-cancer efficacy of cisplatin in H358 cells, where TNF-α does not stimulate the expression of MAPK15. As TNF-α slightly enhances cisplatin-induced cell apoptosis in H1299 cells with stably-overexpressing MAPK15, some other genes induced by TNF-α–NF-κB pathway might be involved in TNF-α-augmented cisplatin-induced cell apoptosis. Overall, manipulation of MAPK15 expression could be a strategy to improve the therapeutic efficacy of cisplatin in the chemotherapy of lung cancer.

Studies have shown that cisplatin exerts its cytotoxic effects by causing DNA crosslinking and subsequently inducing apoptosis in cancer cells (Dasari and Tchounwou, 2014). Thus, we hypothesized that TNF-α–MAPK15 could also exacerbate cisplatin-induced DNA damage. To further verify our hypothesis that TNF-α intensifies cisplatin-induced DNA damage by up-regulating MAPK15, we examined several markers for DNA damage. Persistent phosphorylation of H2AX and cleavage of RAD51 are sensitive indicators for DNA damage (Lu et al., 2006; Leon-Galicia et al., 2018; Yuan et al.,2010). Although previous studies have reported that knockdown of MAPK15 increases the γH2AX foci in breast cancer cells and male germ cell tumors (Groehler and Lannigan, 2010; Rossi et al., 2016), we found no significant increase of p-H2AX in our shMAPK15 H1299 cells. Nevertheless, on cisplatin treatment, the phosphorylation of H2AX and cleavage of RAD51 increased markedly in shCtrl H1299 cells, but not in knockdown MAPK15 cells. Notably, we found that the combination of TNF-α and cisplatin in lung cancer cells caused increased p-H2AX and cleaved RAD51 levels compared to cisplatin alone. Moreover, co-treatment with TNF-α and cisplatin in shCtrl cells caused more severe DNA damage than in knockdown MAPK15 H1299 cells, suggesting that MAPK15 expression facilitates TNF-α-augmented cisplatin-induced DNA damage, further leading to cell apoptosis. On the other hand, an alkaline comet assay was performed to further investigate the role of MAPK15 in cisplatin-induced DNA damage. Our results found that the tail extent moment decreased upon cisplatin treatment in both knockdown MAPK15 and its control H1299 cells, compared with the untreated control group. This indicates that cisplatin bound to DNA and formed DNA-protein crosslinks, which retards DNA mobility and leads to the decrease of tail extent moment (Mendonca et al., 2010; Kosmider et al., 2004; Nesslany et al., 2007). Nevertheless, at 24 h post-treatment with cisplatin, to allow DNA crosslink repair, increased tail extent moment was observed on cisplatin treatment−this method is also used by others to detect DNA crosslink damage and repair (Almeida et al., 2006; Tan et al., 2019). More importantly, our results showed that the DNA repair capacity of knockdown MAPK15 H1299 cells was stronger than that of shCtrl cells on cisplatin treatment, which strongly suggests that MAPK15 expression enhances the efficacy of cisplatin by decreasing DNA repair capacity. In summary, we identified MAPK15 as a critical factor in mediating TNF-α-augmented cisplatin sensitivity, and is potentially involved in cisplatin sensitivity through regulating DNA damage/repair capacity in lung cancer cells (Figure 8). Based on this finding, targeted upregulation of MAPK15 expression might be useful in sensitizing lung cancer cells to cisplatin treatment. TNF-α in combination with lower concentrations of cisplatin has the potential for improving the efficacy of cisplatin, which may contribute to personalized therapeutic strategy.

Limitations of the study

The data reported here address the molecular mechanism of MAPK15 transcriptional upregulation induced by TNF-α and show that the addition of TNF-α can synergize the cisplatin efficacy in lung cancer cells through modulating DNA damage/repair capacity. However, the detailed mechanism of MAPK15 affecting cisplatin-induced DNA damage/repair remains to be determined, and it would be of interest to further explore the relationship of MAPK15 with TNF-α and other chemotherapeutic drugs in the future.

STAR★METHODS

Detailed methods are provided in the online version of this paper and include the following:

- KEY RESOURCES TABLE
- RESOURCE AVAILABILITY
  - Lead contact
  - Materials availability
  - Data and code availability
- EXPERIMENTAL MODEL AND SUBJECT DETAILS
  - Mice

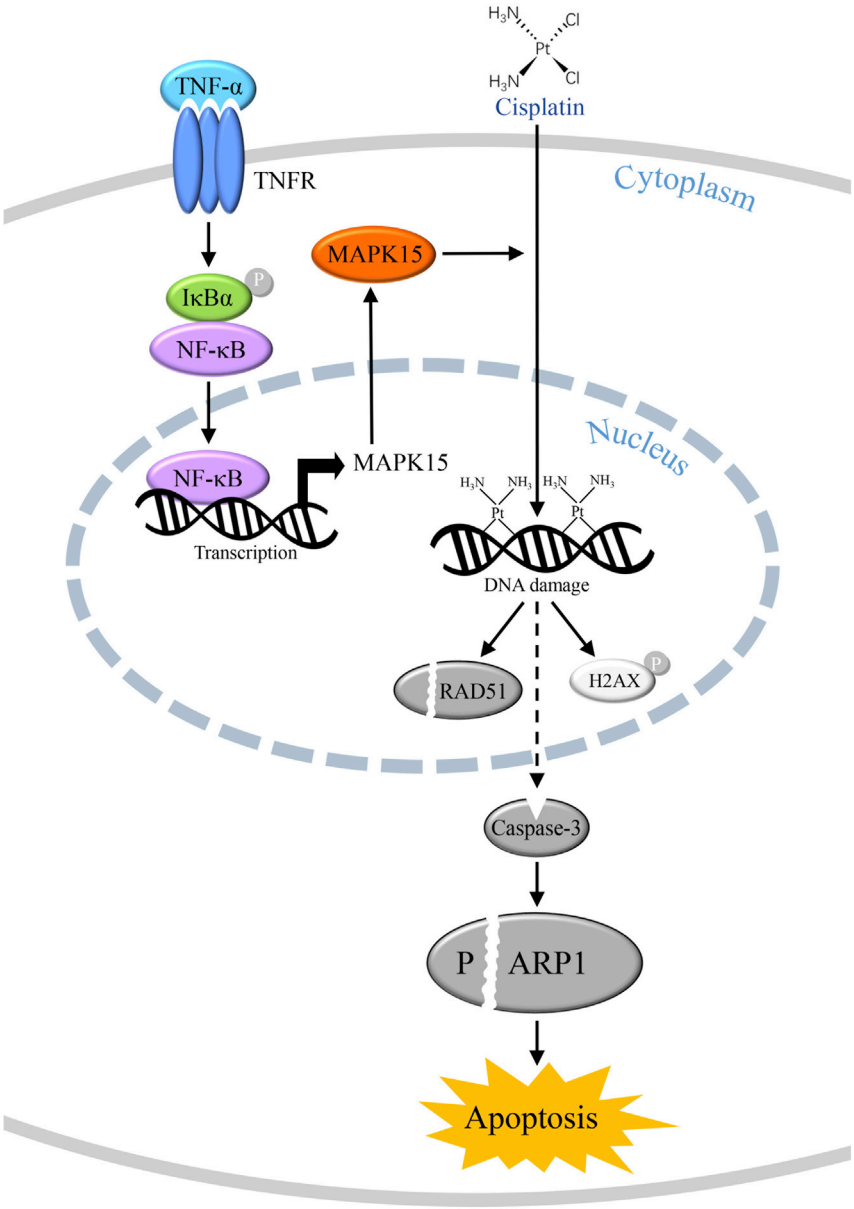

Figure 8. Schematic summary of MAPK15-enhanced sensitivity of human lung cancer cells to cisplatin via TNF-α-activated NF-κB signaling

TNF-α-activated NF-κB signaling initiates the transcription of MAPK15, and the expression of MAPK15 elevates the cellular sensitivity to the chemotherapeutic drug cisplatin through enhancing DNA damage-induced cleavage of RAD51, caspase-3, and PARP1, leading to apoptosis.

- Comet assay
- QUANTIFICATION AND STATISTICAL ANALYSIS

SUPPLEMENTAL INFORMATION

Supplemental information can be found online at https://doi.org/10.1016/j.isci.2022.105459.

ACKNOWLEDGMENTS

We would like to thank members of the Lau and Xu Laboratory for critical comments and Dr. Stanley Lin for English proofreading of this manuscript. This work was supported by the grants from the National Natural Science Foundation of China (31771582, 31900468, and 31271445), the Guangdong Natural Science Foundation of China (2017A030313131), the "Thousand, Hundred, and Ten" Project of the Department of Education of Guangdong Province of China, the Basic and Applied Research Major Projects of Guangdong Province of China (2017KZDXM035 and 2018KZDXM036), the "Yang Fan" Project of Guangdong Province of China (Andy T. Y. Lau-2016 and Yan-Ming Xu-2015), the "Young Innovative Talents" Project of Guangdong Province of China (2019KQNCX034), and the Shantou Medical Health Science and Technology Plan (200624165260857).

AUTHOR CONTRIBUTIONS

D.-D.W., L.-J.D., A.T.Y.L., and Y.-M.X. conceived the study and designed the experiments; D.-D.W. and L.-J.D. performed the majority of the experiments; D.-D.W., L.-J.D., A.T.Y.L., and Y.-M.X. analyzed and interpreted the data with input from H.W.T., X.-Y.Z., Q.-Y.W., Q.-H.Z., Y.-C.J., X.-H.Y., and F.-Y.Y; X.-Y.Z., D.-D.W., and Q.-H.Z. performed the animal experiments; D.-Y.J. and S.-Q.L. provided technical and material supports; D.-D.W., L.-J.D., A.T.Y.L., and Y.-M.X. wrote, reviewed and edited the original draft and revised manuscript; A.T.Y.L. and Y.-M.X. supervised and coordinated the study. All authors read and approved the final version of the manuscript.

DECLARATION OF INTERESTS

The authors declare no conflicts of interest.

Received: March 1, 2022
Revised: August 26, 2022
Accepted: October 24, 2022
Published: December 22, 2022

REFERENCES

Abe, M.K., Saelzler, M.P., Espinosa, R., Kahle, K.T., Hershenson, M.B., Le Beau, M.M., et al. (2002). ERK8, a new member of the mitogen-activated protein kinase family. J. Biol. Chem. *277*, 16733–16743. https://doi.org/10.1074/jbc.M112483200.

Achkar, I.W., Abdulrahman, N., Al-Sulaiti, H., Joseph, J.M., Uddin, S., and Mraiche, F. (2018). Cisplatin based therapy: the role of the mitogen activated protein kinase signaling pathway. J. Transl. Med. *16*, 96. https://doi.org/10.1186/s12967-018-1471-1.

Almeida, G.M., Duarte, T.L., Steward, W.P., and Jones, G.D. (2006). Detection of oxaliplatin-induced DNA crosslinks in vitro and in cancer patients using the alkaline comet assay. DNA Repair *5*, 219–225. https://doi.org/10.1016/j.dnarep.2005.09.010.

Benedetti, G., Fredriksson, L., Herpers, B., Meerman, J., van de Water, B., and de Graauw, M. (2013). TNF-alpha-mediated NF-kappaB survival signaling impairment by cisplatin enhances JNK activation allowing synergistic apoptosis of renal proximal tubular cells. Biochem. Pharmacol. *85*, 274–286. https://doi.org/10.1016/j.bcp. 2012.10.012.

Bray, F., Ferlay, J., Soerjomataram, I., Siegel, R.L., Torre, L.A., and Jemal, A. (2018). Global cancer statistics 2018: GLOBOCAN estimates of incidence and mortality worldwide for 36 cancers in 185 countries. CA Cancer J. Clin. *68*, 394–424. https://doi.org/10.3322/caac.21492.

Cai, N.L., Lau, A.T.Y., Yu, F.Y., Wu, D.D., Dai, L.J., Mo, H.Y., et al. (2017). Purification and characterization of a highly specific polyclonal antibody against human extracellular signal-regulated kinase 8 and its detection in lung cancer. PLoS One *12*, e0184755. https://doi.org/10.1371/journal.pone.0184755.

Dasari, S., and Tchounwou, P.B. (2014). Cisplatin in cancer therapy: molecular mechanisms of action. Eur. J. Pharmacol. *740*, 364–378. https://doi.org/10.1016/j.ejphar.2014. 07.025.

Fennell, D.A., Summers, Y., Cadranel, J., Benepal, T., Christoph, D.C., Lal, R., et al. (2016). Cisplatin in the modern era: the backbone of first-line chemotherapy for non-small cell lung cancer. Cancer Treat. Rev. *44*, 42–50. https://doi.org/10.1016/j.ctrv.2016.01.003.

Galenkamp, K.M., Carriba, P., Urresti, J., Planells-Ferrer, L., Coccia, E., Lopez-Soriano, J., et al. (2015). TNF alpha sensitizes neuroblastoma cells to FasL-, cisplatin- and etoposide-induced cell death by NF-kappaB-mediated expression of Fas. Mol. Cancer *14*, 62. https://doi.org/10.1186/s12943-015-0329-x.

Galluzzi, L., Senovilla, L., Vitale, I., Michels, J., Martins, I., Kepp, O., et al. (2012). Molecular mechanisms of cisplatin resistance. Oncogene *31*, 1869–1883. https://doi.org/10.1038/onc.2011.384.

Galluzzi, L., Vitale, I., Michels, J., Brenner, C., Szabadkai, G., Harel-Bellan, A., et al. (2014). Systems biology of cisplatin resistance: past, present and future. Cell Death Dis. *5*, e1257. https://doi.org/10.1038/cddis.2013.428.

Groehler, A.L., and Lannigan, D.A. (2010). A chromatin-bound kinase, ERK8, protects genomic integrity by inhibiting HDM2-mediated degradation of the DNA clamp PCNA. J. Cell

Biol. *190*, 575–586. https://doi.org/10.1083/jcb.201002124.

Hayden, M.S., and Ghosh, S. (2008). Shared principles in NF-kappa B signaling. Cell *132*, 344–362. https://doi.org/10.1016/j.cell.2008.01.020.

Hayden, M.S., and Ghosh, S. (2014). Regulation of NF-κB by TNF family cytokines. Semin. Immunol. *26*, 253–266. https://doi.org/10.1016/j.smim.2014.05.004.

Henrich, L.M., Smith, J.A., Kitt, D., Errington, T.M., Nguyen, B., Traish, A.M., et al. (2003). Extracellular signal-regulated kinase 7, a regulator of hormone-dependent estrogen receptor destruction. Mol. Cell. Biol. *23*, 5979–5988. https://doi.org/10.1128/mcb.23.17.5979–88.2003.

Iavarone, C., Acunzo, M., Carlomagno, F., Catania, A., Melillo, R.M., Carlomagno, S.M., et al. (2006). Activation of the Erk8 mitogen-activated protein (MAP) kinase by RET/PTC3, a constitutively active form of the RET proto-oncogene. J. Biol. Chem. *281*, 10567–10576. https://doi.org/10.1074/jbc. M513397200.

Klevernic, I.V., Stafford, M.J., Morrice, N., Peggie, M., Morton, S., and Cohen, P. (2006). Characterization of the reversible phosphorylation and activation of ERK8. Biochem. J. *394*, 365–373. https://doi.org/10.1042/BJ20051288.

Klevernic, I.V., Martin, N.M., and Cohen, P. (2009). Regulation of the activity and expression of ERK8 by DNA damage. FEBS Lett. *583*, 680–684. https://doi.org/10.1016/j.febslet.2009. 01.011.

Kosmider, B., Wyszynska, K., Janik-Spiechowicz, E., Osiecka, R., Zyner, E., Ochocki, J., et al. (2004). Evaluation of the genotoxicity of cis-bis(3-aminoflavone) dichloroplatinum (II) in comparison with cis-DDP. Mutat. Res. *558*, 93–110. https://doi.org/10.1016/j. mrgentox.2003.11.006.

Lau, A.T.Y., and Xu, Y.M., (2019). Regulation of human mitogen-activated protein kinase 15 (extracellular signal-regulated kinase 7/8) and its functions: a recent update. J. Cell. Physiol. *234*, 75–88. https://doi.org/10.1002/jcp.27053.

Leon-Galicia, I., Diaz-Chavez, J., Albino-Sanchez, M.E., Garcia-Villa, E., Bermudez-Cruz, R., Garcia-Mena, J., et al. (2018). Resveratrol decreases Rad51 expression and sensitizes cisplatin-resistant MCF-7 breast cancer cells. Oncol. Rep. *39*, 3025–3033. https://doi.org/10.3892/or.2018.6336.

Livak, K.J., and Schmittgen, T.D. (2001). Analysis of relative gene expression data using real-time quantitative PCR and the 2(-Delta Delta C(T)) Method. Methods *25*, 402–408. https://doi.org/10.1006/meth.2001.1262.

Lu, C., Zhu, F., Cho, Y.Y., Tang, F., Zykova, T., Ma, W.Y., et al. (2006). Cell apoptosis: requirement of H2AX in DNA ladder formation, but not for the activation of caspase-3. Mol. Cell *23*, 121–132. https://doi.org/10.1016/j.molcel.2006.05.023.

Mendonca, L.M., dos Santos, G.C., dos Santos, R.A., Takahashi, C.S., Bianchi, M. de.L., and Antunes, L.M. (2010). Evaluation of curcumin and cisplatin-induced DNA damage in PC12 cells by the alkaline comet assay. Hum. Exp. Toxicol. *29*, 635–643. https://doi.org/10.1177/0960327109358731.

Miller, K.D., Nogueira, L., Mariotto, A.B., Rowland, J.H., Yabroff, K.R., Alfano, C.M., et al. (2019). Cancer treatment and survivorship statistics. CA Cancer J. Clin. *69*, 363–385. https://doi.org/10.3322/caac. 21565.

Nesslany, F., Zennouche, N., Simar-Meintieres, S., Talahari, I., NKili-Mboui, E.N., and Marzin, D. (2007). In vivo Comet assay on isolated kidney cells to distinguish genotoxic carcinogens from epigenetic carcinogens or cytotoxic compounds. Mutat. Res. *630*, 28–41. https://doi.org/10.1016/j.mrgentox.2007.02.010.

Oeckinghaus, A., Hayden, M.S., and Ghosh, S. (2011). Crosstalk in NF-kappaB signaling pathways. Nat. Immunol. *12*, 695–708. https://doi.org/10.1038/ni.2065.

Olive, P.L., and Banath, J.P. (2006). The comet assay: a method to measure DNA damage in individual cells. Nat. Protoc. *1*, 23–29. https://doi.org/10.1038/nprot.2006.5.

Ramesh, G., and Reeves, W.B. (2002). TNF-alpha mediates chemokine and cytokine expression and renal injury in cisplatin nephrotoxicity. J. Clin. Invest. *110*, 835–842. https://doi.org/10.1172/JCI15606.

Ramesh, G., and Reeves, W.B. (2003). TNFR2-mediated apoptosis and necrosis in cisplatin-induced acute renal failure. Am. J. Physiol. Renal Physiol. *285*, F610–F618. https://doi.org/10.1152/ajprenal.00101.2003.

Rossi, M., Colecchia, D., Iavarone, C., Strambi, A., Piccioni, F., Verrotti di Pianella, A., et al. (2011). Extracellular signal-regulated kinase 8 (ERK8) controls estrogen-related receptor α (ERRα) cellular localization and inhibits its transcriptional activity. J. Biol. Chem. *286*, 8507–8522. https://doi.org/10.1074/jbc.M110.179523.

Rossi, M., Colecchia, D., Ilardi, G., Acunzo, M., Nigita, G., Sasdelli, F., et al. (2016). MAPK15 upregulation promotes cell proliferation and prevents DNA damage in male germ cell tumors. Oncotarget *7*, 20981–20998. https://doi.org/10.18632/oncotarget.8044.

Saelzler, M.P., Spackman, C.C., Liu, Y., Martinez, L.C., Harris, J.P., and Abe, M.K. (2006). ERK8 down-regulates transactivation of the glucocorticoid receptor through Hic-5. J. Biol. Chem. *281*, 16821–16832. https://doi.org/10.1074/jbc.M512418200.

Sullivan, I., Salazar, J., Majem, M., Pallarés, C., Del Río, E., Páez, D., et al. (2014). Pharmacogenetics of the DNA repair pathways in advanced non-small cell lung cancer patients treated with platinum-based chemotherapy. Cancer Lett. *353*, 160–166. https://doi.org/10.1016/j.canlet.2014.07.023.

Tan, H.W., Liang, Z.L., Yao, Y., Wu, D.D., Mo, H.Y., Gu, J., et al. (2019). Lasting DNA damage and aberrant DNA repair gene expression profile are associated with post-chronic cadmium exposure in human bronchial epithelial cells. Cells *8*, 842–863. https://doi.org/10.3390/cells8080842.

Wang, X., Martindale, J.L., and Holbrook, N.J. (2000). Requirement for ERK activation in cisplatin-induced apoptosis. J. Biol. Chem. *275*, 39435–39443. https://doi.org/10.1074/jbc.M004583200.

Wu, D.D., Lau, A.T.Y., Yu, F.Y., Cai, N.L., Dai, L.J., Kim, M.O., et al. (2017a). Extracellular signal-regulated kinase 8-mediated NF-κB activation increases sensitivity of human lung cancer cells to arsenic trioxide. Oncotarget *8*, 49144–49155. https://doi.org/10.18632/oncotarget.17100.

Wu, X., Wu, M., Jiang, M., Zhi, Q., Bian, X., Xu, M., et al. (2017b). TNF-alpha sensitizes chemotherapy and radiotherapy against breast cancer cells. Cancer Cell Int. *17*, 13. https://doi.org/10.1186/s12935-017-0382-1.

Xu, Y.M., Zhu, F., Cho, Y.Y., Carper, A., Peng, C., Zheng, D., et al. (2010). Extracellular signal-regulated kinase 8-mediated c-Jun phosphorylation increases tumorigenesis of human colon cancer. Cancer Res. *70*, 3218–3227. https://doi.org/10.1158/0008-5472.CAN-09-4306.

Yuan, J., Adamski, R., and Chen, J. (2010). Focus on histone variant H2AX: to be or not to be. FEBS Lett. *584*, 3717–3724. https://doi.org/10.1016/j.febslet.2010.05.021.

Zhang, B., Ramesh, G., Norbury, C.C., and Reeves, W.B. (2007). Cisplatin-induced nephrotoxicity is mediated by tumor necrosis factor-α produced by renal parenchymal cells. Kidney Int. *72*, 37–44. https://doi.org/10.1038/sj.ki.5002242.

STAR★METHODS

KEY RESOURCES TABLE

REAGENT or RESOURCE	SOURCE	IDENTIFIER
Antibodies		
MAPK15 antibody	Cai et al., 2017	N/A
NF-κB p65 antibody	Cell Signaling Technology	Cat#8242
Caspase-3 antibody	GeneTex	GTX110543
PARP1 antibody	GeneTex	GTX100573
Xpress antibody	Invitrogen	Cat#46-0528
IκBα antibody	BBI Life Sciences	AB20138a
p-H2AX antibody	ABclonal	AP0099
H2AX antibody	ABclonal	A11361
RAD51 antibody	GeneTex	GTX100469
p21 antibody	BBI Life Sciences	D120403
p-p44/42 MAPK (ERK1/2) (Thr202/Tyr204) antibody	Cell Signaling Technology	Cat#4370
ERK1/2 (H-72) antibody	Santa Cruz Biotechnology	sc-292838
β-Actin antibody	Sigma Aldrich	A5441
Anti-mouse IgG-HRP antibody	Santa Cruz Biotechnology	sc-2005
Anti-rabbit IgG-HRP antibody	Santa Cruz Biotechnology	sc-2004
Chemicals, peptides, and recombinant proteins		
TNF-α	PeproTech	Cat#300-01A
JSH-23	Selleck	S7351
Cisplatin	Haosen Pharmaceutical Industry	N/A
Critical commercial assays		
Chromatin IP Kit	Cell Signaling Technology	Cat#9003
Biotin 3′ End DNA Labeling Kit	Thermo Fisher Scientific	Cat#89818
LightShift Chemiluminescent Electrophoretic mobility shift assay (EMSA) kit	Thermo Fisher Scientific	Cat#20148
NE-PER Reagents	Thermo Fisher Scientific	Cat#78835
Dual-Luciferase® Reporter Assay kit	Promega	E1960
qPCR master mix	Promega	A6001
Experimental models: Cell lines		
NCI-H1299	ATCC	CRL-5803
NCI-H460	ATCC	HTB-177
NCI-H358	ATCC	CRL-5807
Software		
GraphPad Prism 7	GraphPad Software	https://www.graphpad.com/
Oligonucleotides		
Primer sequences are listed in Table S2		

RESOURCE AVAILABILITY

Lead contact

The additional data collected in our study are available from the corresponding author on reasonable request. Yan-Ming Xu (amyymxu@stu.edu.cn).

Materials availability

Plasmids and antibody generated in this study will be available on request.

Data and code availability

- All data reported in this article will be shared by the lead contact on request.
- This article does not report original code.
- Any additional information required to reanalyze the data reported in this article is available from the lead contact on request.

EXPERIMENTAL MODEL AND SUBJECT DETAILS

Mice

Six- to eight-week-old BALB/c male nude mice were purchased from Beijing Vital River Laboratory Animal Technology Co., Ltd. Mice were maintained under specific pathogen-free conditions and received humane care according to the Shantou University Medical College Institutional Animal Care and Treatment Committee.

To assess the growth of tumor xenografts, stably overexpressing MAPK15 or control H1299 cells were suspended in a total volume of 200 μL DPBS (5×10^6 cells) and subcutaneously injected into the two flanks of BALB/c nude mice, one cell line on each side. Tumor size was measured using a caliper on Day 31 after inoculation. To evaluate cisplatin sensitivity *in vivo*, BALB/c nude mice were administered with 3.5 mg/kg cisplatin peritumorally at 31 days after cell injection and the treatment was repeated twice a week. Tumor volume was calculated using the formula length×width^2/2, and the tumor tissues were removed on the last day.

To explore the effect of TNF-α on cisplatin treatment, H1299 cells were subcutaneously injected into the two flanks of BALB/c nude mice (5×10^6 cells in 200 μL DPBS). Beginning 31 days after inoculation, mice twice a week were given an intraperitoneal injection of TNF-α (20 ng) followed 12 h later with a peritumoral injection of 3.5 mg/kg cisplatin. The control groups were injected with an equal volume of saline. Treatment was conducted repeatedly and continuously for 14 days.

Cell culture

Human lung cancer cell lines H1299, H460, and H358 were maintained in RPMI 1640 with 10% fetal bovine serum and 1% penicillin and streptomycin. Cell viability was measured by a naphthol blue black (NBB) assay as described previously (Wu et al., 2017a). In brief, cells were fixed with 4% formaldehyde at room temperature for 8 min and stained with 0.05% NBB solution (0.05% NBB, 9% acetic acid, 0.1 M sodium acetate) for 30 min. After staining, cells were washed with distilled water thrice, and eluted with 50 mM NaOH after air-drying. The absorbance was measured at 595 nm using a Thermo Scientific Multiskan FC (Thermo Scientific, USA).

METHOD DETAILS

Plasmids, antibodies, and reagents

The antibodies and reagents are listed in the key resources table.

Construction of plasmids and stable cell lines

Plasmids pcDNA4/Xpress-MAPK15, pCMV4/3HA-IκBα, and pCMV-p65 were described previously (Wu et al., 2017a). Transfection was performed when cell confluence reached 70–80% and 6 μg of total plasmids was transfected into cells with 15 μL polyethylenimine (PEI) transfection reagent (ratio 1:2.5). Stable shMAPK15 and shRNA scrambled control H1299 cell lines were generated as previously described (Wu et al., 2017a). MAPK15 shRNA plasmid (h) (sc-77462-SH, Santa Cruz Biotechnology, Santa Cruz, CA) is a target-specific lentiviral vector plasmid encoding a 19–25 nt (plus hairpin) shRNA for knocking down gene expression. Control shRNA plasmid-A (sc-108060) encodes a scrambled shRNA sequence. Stably overexpressing MAPK15 and empty vector control H1299 cell lines were selected in Zeocin for 14 days after transfection of pcDNA4-MAPK15 or the empty vector pcDNA4.

Quantitative real-time RT-PCR (qRT-PCR)

Total RNA was extracted from cells using TRIzol reagent (Thermo Fisher Scientific, 15596018). cDNA was synthesized with a PrimeScript Reverse Transcriptase kit (Takara, 2680A) following the manufacturer's instructions. qRT-PCR was performed on an Applied Biosystems 7500 Real-Time PCR System with GoTaq qPCR Master Mix (A6001) from Promega (Fitchburg, WI), and gene-specific primers were synthesized by Guangzhou IGE Biotechnology with the following sequences: MAPK15 (forward: 5′-GACCAGA AGCCGTCCAATGT-3′; reverse: 5′-GTATCGGTGCGAAGAGAGCA-3′), IκBα (forward: 5′-GCTCCGAGAC TTTCGAGGAA-3′; reverse: 5′-ACGTGTGGCCATTGTAGTTG-3′), β-actin (forward: 5′-ATGGGTCAGAAGG ATTCCTATGTG-3′; reverse: 5′-CTTCATGAGGTAGTCAGTCAGGTC-3′). β-Actin was amplified as the internal control to normalize gene expression. qRT-PCR data were analyzed using 7500 software v2.0.6 and relative expression of target genes was calculated by the $2^{-\Delta\Delta CT}$ method (Livak and Schmittgen, 2001).

Immunoblot assay

Cells were washed thrice with ice-cold phosphate-buffered saline (PBS) and lysed with sample buffer (62.5 mM Tris-Cl [pH 8.8], 2% SDS, 10% glycerol, 0.1 M DTT, 0.01% bromophenol blue). Protein samples were subjected to 10% SDS-PAGE and transferred onto PVDF membranes. The membrane was blocked with 5% nonfat dry milk in Tris-buffered saline containing 0.1% Tween 20, and then incubated with primary antibody at 4°C overnight. After incubation with horseradish peroxidase-conjugated secondary antibodies, proteins were detected via an enhanced chemiluminescence reagent.

Chromatin immunoprecipitation (ChIP) assay

NF-κB binding sites on the promoter of MAPK15 were predicted via the JASPAR website (http://jaspar.genereg.net/). To validate the binding affinity of NF-κB to the MAPK15 promoter *in vivo*, ChIP assay was performed using a SimpleChIP Enzymatic Chromatin IP Kit (Cell Signaling Technology, Boston, MA) in accordance with the manufacturer's instructions. Briefly, H1299 cells were crosslinked with 1% formaldehyde for 10 min at room temperature, then harvested and incubated on ice for 30 min in lysis buffers. Nuclei were pelleted by centrifugation, digested with micrococcal nuclease, and stopped by adding 0.5 M EDTA. Following sonication and centrifugation, sheared chromatin was incubated with NF-κB p65 antibody (8242; Cell Signaling Technology) or normal rabbit IgG (negative control) at 4°C overnight. Protein G magnetic beads were added and incubated for another 2 h. Antibody-bound protein-DNA complexes were subjected to DNA purification and analyzed by PCR. The primers for RT-PCR were synthesized in Guangzhou IGE Biotechnology company (Table S2). RT-PCR Amplification products were subjected to 2% agarose gel electrophoresis.

Electrophoretic mobility shift assay (EMSA)

EMSA was performed to verify the binding ability of NF-κB to the MAPK15 promoter *in vitro*. Nuclear extracts of H1299 cells transiently transfected with pCMV-p65 were isolated using the NE-PER Nuclear and Cytoplasmic Extraction reagent kit (Thermo Fisher Scientific). Biotin-labeled MAPK15 promoter DNA probes were prepared using the Biotin 3′ End DNA Labeling Kit (Thermo Fisher Scientific). Probe sequences were: forward: 5′-TAAATGTGTATTTCCATTATCCCCC-3′; reverse: 5′-GGGGGATAATGGAAA TACACATTTA-3′. In brief, biotin-labeled MAPK15 promoter DNA probes (20 fmol) and nuclear extracts (2 μg) were reacted in 20 μL binding buffer for 20 min at room temperature. After the reaction, the samples were subjected to 5% native PAGE, transferred onto a nylon membrane, and crosslinked to the membrane via UV irradiation. The biotin-labeled probe was detected with streptavidin-horseradish peroxidase. The control group consisted of 200-fold excess unlabeled cold probe.

Dual-luciferase reporter gene assay

A luciferase reporter gene driven by five repeated TBS4 MAPK15 binding sites, in the promoter, was constructed from pUC19-5×MAPK15 site4, synthesized by Guangzhou IGE Biotechnology, and inserted into the pJC6-GL3-firefly luciferase plasmid between the *Afl II* and *Nsi I* site. The resulting recombinant plasmid was named pJC6-GL3-5×MAPK15-firefly. Mutations of TBS4 (gggaatatcg) were cloned into pJC6-GL3-firefly luciferase reporter by replacing 5×TBS4 MAPK15 binding sites (gtgtatttcc). Mutant 1: five repeats; Mutant 2: seven repeats.

Firefly luciferase plasmid (pJC6-GL3-5×MAPK15-firefly), or its mutants, and *Renilla* luciferase plasmid (pRL-SV40p-*Renilla*) were co-transfected into H1299 cells using PEI. After treatment, cells were lysed

with passive lysis buffer (Dual-Luciferase Reporter Assay System, Promega) at room temperature for 30 min by gentle shaking, and then firefly luciferase activity was measured. The MAPK15 firefly luciferase activity was normalized against *Renilla* luciferase activity (pRL-SV40p-*Renilla*).

Cell cycle flow cytometric analysis

Cells after TNF-α and/or cisplatin treatment were trypsinized, washed thrice with Dulbecco's PBS (DPBS), and fixed with pre-chilled 70% ethanol, cells were then stained with propidium iodide (PI) containing RNase for 15 min. For cell cycle analysis, cells were analyzed using a BD Accuri C6 flow cytometer (BD Bioscience, San Diego, USA).

Comet assay

Comet assay, a single-cell gel electrophoresis, was used to assess DNA damage and DNA repair capacity as described previously (Tan et al., 2019; Olive and Banath, 2006). Images were captured using a fluorescence microscope (Axiovert 40 CFL) with a digital camera (QImaging Micro-Publisher 5.0 RTV) and viewed by the accompanying software QCapture (v2.9.13, Quantitative Imaging Corp.). Individual images were analyzed using the Comet Assay Software Project software (v1.2.3b2, CaspLab), and 50 to 100 non-overlapping cells per sample were analyzed. The means of the % tail DNA and tail extent moment from three separate experiments were calculated as levels of DNA damage. The tail extent moment is defined as "% tail DNA × comet tail length ÷ 100".

QUANTIFICATION AND STATISTICAL ANALYSIS

Experimental results were analyzed with GraphPad Prism 7 software. Two-way ANOVA was used to compare data between groups and a multiple *t*-test was used to compare data among groups. *$p<0.05$ was considered to indicate statistical significance.